
Solving Over-Smoothing in GNNs via Nonlocal Message Passing: Algebraic Smoothing and Depth Scalability

WeiQi Guan*

wqguan24@m.fudan.edu.cn

Junlin He†

junlinspeed.he@connect.polyu.hk

Abstract

The relationship between Layer Normalization (LN) placement and the over-smoothing phenomenon remains underexplored. We identify a critical dilemma: **Pre-LN** architectures avoid over-smoothing but suffer from the *curse of depth*, while **Post-LN** architectures bypass the curse of depth but experience over-smoothing.

To resolve this, we propose a new method based on Post-LN that induces algebraic smoothing, preventing over-smoothing without the curse of depth. Empirical results across five benchmarks demonstrate that our approach supports deeper networks (up to 256 layers) and improves performance, requiring no additional parameters.

Key contributions:

- **Theoretical Characterization:** Analysis of LN dynamics and their impact on over-smoothing and the curse of depth.
- **A Principled Solution:** A parameter-efficient method that induces algebraic smoothing and avoids over-smoothing and the curse of depth.
- **Empirical Validation:** Extensive experiments showing the effectiveness of the method in deeper GNNs.

1 Introduction

Graph Neural Networks (GNNs) have emerged as the de facto standard for learning from graph-structured data, ranging from motif detection (Besta et al., 2022) to social network analysis (Fan et al., 2019). Despite their widespread success, GNNs face a fundamental limitation regarding their depth: *over-smoothing*. This phenomenon manifests as the exponential convergence of node representations to a distinguishing-less subspace as the number of layers increases, leading to severe performance degradation in deep architectures. While foundational models such as Graph Convolutional Networks (GCN) (Kipf and Welling, 2017) and Graph Attention Networks (GAT) (Veličković et al., 2018) remain dominant baselines (Luo et al., 2024), they are theoretically susceptible to such issue (Wu et al., 2023b; Oono and Suzuki, 2020; Cai and Wang, 2020).

Significant research efforts have been dedicated to mitigating over-smoothing (Chen et al., 2020a; Zhao and Akoglu, 2020; Scholkemper et al., 2025), particularly through the lens of differential equation analysis. Notably, GNNs can be interpreted as discretizations of continuous differential equations, with foundational works establishing connections to heat equations and diffusion processes (Chamberlain et al., 2021; Wu et al., 2019). While refining the discretization step size allows for deeper architectures, it fails to fundamentally prevent the exponential decay of Dirichlet energy associated with diffusive dynamics. Consequently, recent studies have sought to identify dynamical

*School of Mathematical Sciences, Fudan University, Shanghai 200433, China

†Corresponding author

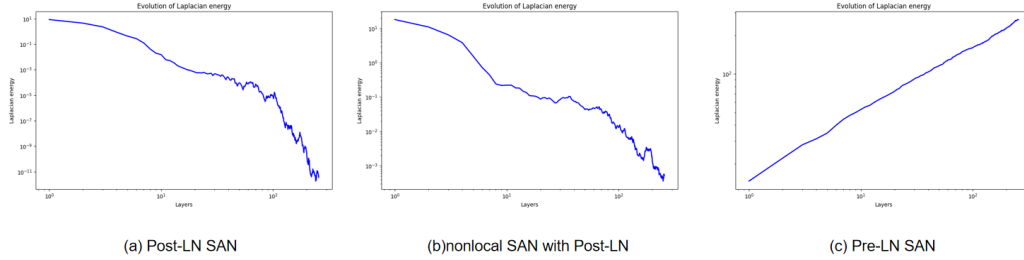


Figure 1: Log-log plots of Laplacian energy evolution at initialization on Cora. The panels display (a) the Post-LN SAN, (b) our proposed nonlocal SAN with Post-LN, and (c) the Pre-LN SAN architecture.

systems that inherently avoid such decay. Pioneering work by Rusch et al. (2022) introduced wave equations on graphs, which exhibit oscillatory behavior rather than converging exponentially to a steady state. Subsequently, Rusch et al. (2023b) incorporated a gradient gating mechanism to achieve algebraically smoothing, while Kang et al. (2024) recently leveraged fractional time derivatives to attain similar effects. However, a critical limitation persists across these methods: the reliance on layer-shared edge weights (time-invariant parameters). This architectural constraint—prevalent in both explicit schemes (Rusch et al., 2023b) and implicit schemes where the step size functions as the layer index (Rusch et al., 2022; Kang et al., 2024)—substantially limits the model’s representational capacity and flexibility.

Inspired by the transformative success of Large Language Models (LLMs) (Vaswani et al., 2017), which can be conceptually viewed as models operating on fully-connected graphs, researchers have increasingly adapted the Transformer architecture to graph data to capture long-range dependencies (Rampášek et al., 2023; Shirzad et al., 2023; Wu et al., 2023a). Since Transformers can be formally viewed as fully connected GNNs employing self-attention (Joshi, 2025), it is natural to investigate whether they inherit the over-smoothing pathologies of traditional GNNs. A critical component governing the signal propagation and trainability of Transformers is Layer Normalization (LN). Extensive research in the NLP domain has revealed that the placement of LN—specifically Pre-LN versus Post-LN configurations—dramatically impacts model convergence and stability (Wang et al., 2019; Chen et al., 2020b). For instance, Pre-LN is often associated with better training stability but suffers from the *curse of depth*, a phenomenon first formalized in (Sun et al., 2025). This term describes the observation where deeper layers in modern LLMs contribute significantly less to representation learning compared to earlier ones. In contrast, while Post-LN architectures can lead to rank collapse or convergence to a single cluster (Shi et al., 2022; Geshkovski et al., 2025), they appear immune to the curse of depth, although this property has primarily been empirically observed in shallow configurations (Sun et al., 2025).

Despite these insights in LLMs, the direct causal relationship between Layer Normalization placement and the over-smoothing phenomenon specifically within attention-based GNNs remains largely unexplored. Surprisingly, we find a critical dilemma: **Pre-LN** configurations succumb to the *curse of depth* despite avoiding signal collapse (over-smoothing), whereas **Post-LN** architectures avoid the curse of depth but suffer from rapid *over-smoothing*. Figure 1(c) reveals a power-law scaling of Laplacian energy in **Pre-LN** architectures, a behavior driven by the dominance of residual connections in the signal propagation. Although this mechanism averts the collapse of Laplacian energy (over-smoothing), it induces a side effect called *curse of depth*: representations undergo minimal evolution across layers, as corroborated by the high inter-layer cosine similarity in Figure 2(b). In sharp contrast, **Post-LN** architectures place greater emphasis on the residual branch, which serves to diversify features across layers. Nevertheless, they suffer from an exponential decay of high-frequency components as shown in Figure 1(a), a phenomenon that leads to the over-smoothing issue. These observations align with those reported in LLMs (Sun et al., 2025; Shi et al., 2022; Geshkovski et al., 2025).

To rigorously analyze the layer-wise behavior of GNNs, we establish a novel theoretical framework by modeling GNNs as generalized weighted graphs and employing integration by parts tools. Within this

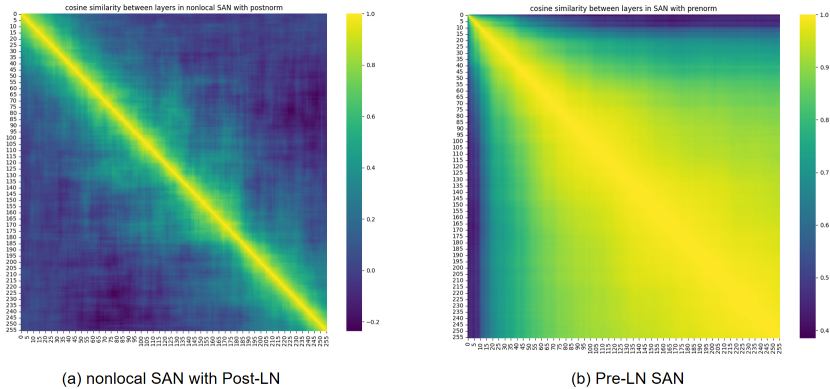


Figure 2: Inter-layer cosine similarity of representations after training on Cora. (a) Our proposed nonlocal SAN with Post-LN. (b) The Pre-LN SAN.

framework, we first demonstrate that the weighted aggregation operation inherent in standard GNNs inevitably leads to over-smoothing, characterized by an exponential decay of the Laplacian energy as the network depth increases. Furthermore, we extend our analysis to the Pre-LN configuration. While the property that the Laplacian energy exhibits a power-law growth pattern renders Pre-LN architectures robust against over-smoothing, we identify a critical limitation: the relative Laplacian energy decays to zero. This estimate of decay precipitates the curse of depth, hindering the effective training of extremely deep networks. To resolve this dilemma, we turn our attention to the Post-LN architecture, which naturally avoids the curse of depth but traditionally suffers from over-smoothing. Building upon Post-LN, we propose a principled method with formal guarantees that enforces a power-law decay of the Laplacian energy. This approach achieves algebraic smoothing, thereby fundamentally mitigating the over-smoothing issue without introducing the optimization difficulties associated with the curse of depth. As illustrated in Figure 1(b), the Laplacian energy in our model decays slowly, maintaining a significant magnitude of 10^{-5} even at a depth of 256 layers. Crucially, our proposed method effectively circumvents the curse of depth, as corroborated by the low inter-layer cosine similarity shown in Figure 2(a). Extensive experiments validate both our theoretical analysis and the superiority of the proposed method. Our main contributions are summarized as follows:

- **Theoretical Characterization of LN Dynamics:** We perform a systematic investigation into the impact of Layer Normalization (LN) placement on the dichotomy between *over-smoothing* and the *curse of depth*. Within a theoretical framework based on weighted graphs, we provide a formal analysis using integration by parts to delineate the asymptotic behaviors of Laplacian energy.
- **A Principled Remedy for Over-smoothing:** We propose a novel, parameter-efficient, and theoretically guaranteed method called nonlocal message passing to fundamentally overcome over-smoothing in Post-LN architectures. By inducing algebraic smoothing rather than exponential decay, our method requires no additional parameters and incurs negligible computational overhead. Importantly, our model remains immune to the curse of depth.
- **Empirical Verification and Scalability:** We conduct comprehensive experiments across 5 benchmarks to corroborate our theoretical findings. The empirical results demonstrate that our method effectively mitigates the over-smoothing issue, enabling the successful training of significantly deeper networks (up to at least 256 layers), avoiding the curse of depth, improving performance.

2 Preliminaries

In this section, we review the fundamental analysis on weighted undirected graphs $G = (V, E, \omega, \mu)$. The graph structure consists of a vertex set V , an edge set E , a symmetric weight function ω on E satisfying $\omega_{ij} = \omega_{ji} > 0$ for every $(i, j), (j, i) \in E$, and a vertex measure μ on V with $\mu(i) > 0$ for all $i \in V$, we also abbreviate $\mu(i)$ as μ_i . Denote n as the number of nodes. If node j is a neighborhood

of node i , we denote as $i \sim j$. The neighborhood of node i is denoted as $\mathcal{N}_i := \{j \in [n] : j \sim i\}$. The space of vector-valued functions on G is denoted by $C(G) = \{X : V \rightarrow \mathbb{R}^d\}$. Readers may be more familiar with the expression for features on graphs as matrix $X \in \mathbb{R}^{n \times d}$, and can view $X(i)$ as the i -th row vectors and $u(i, j)$ as (i, j) elements in matrix X . For two functionals $\mathcal{E}_1, \mathcal{E}_2 : C(G) \rightarrow \mathbb{R}$ we denote $\mathcal{E}_1 \sim \mathcal{E}_2$ if there exist universal constants C_1, C_2 such that $C_1 \mathcal{E}_1(X) \leq \mathcal{E}_2(X) \leq C_2 \mathcal{E}_1(X)$ for all $X \in C(G)$. For any $X \in C(G)$, the weighted Laplacian is defined as

$$\Delta_\mu X(i) = \sum_{j \sim i} \frac{\omega_{ij}}{\mu_i} (X(j) - X(i)).$$

Readers can also view weighted Laplacian as $n \times n$ matrix, two views are the same thing. If $\sum_{j \in \mathcal{N}_i} \omega_{ij} < \mu_i$, then we define the aggregation matrix as $P_\mu = \Delta_\mu + I_n$ with I_n the identity matrix. For $X \in C(G)$, we define the integration of X as

$$\int_G X d\mu = \sum_{i \in [n]} X(i) \mu_i.$$

For any $X, Y \in C(G)$, we define the inner product of gradient as follows.

$$\nabla_\mu X \cdot \nabla_\mu Y(i) = \sum_{j \sim i} \frac{\omega_{ij}}{\mu_i} (X(j) - X(i)) \cdot (Y(j) - Y(i)).$$

We abbreviate $\nabla_\mu X \cdot \nabla_\mu X$ as $|\nabla_\mu X|^2$. For a vector $p = (p_1, \dots, p_d)$, the l^2 norm of vector p is defined as $|p| = \sqrt{\sum_{i=1}^d p_i^2}$. For $X \in C(G)$, We define $\|X\|$ as

$$\|X\| = \sqrt{\sum_{i \in [n]} |X(i)|^2}$$

The update rule for attention-based GNNs is given by

$$X^{k+1} = \sigma(P^k X^k W^k).$$

Where W^k is a learnable weight matrix and P^k is the aggregation matrix at the k -th layer. Let P_{ij}^k be the element in the i -th row and j -th column of P^k , which represents the attention value of the edge (x_i, x_j) . In attention-based GNNs, P_{ij}^k is defined as:

$$P_{ij}^k = \frac{\exp(e_{ij}^k)}{\exp(e_{ii}^k) + \sum_{l \in \mathcal{N}_i} \exp(e_{il}^k)}.$$

where $e_{ij}^k = g^k(X_i^k, X_j^k, \theta_{ij}^k)$ with learnable parameters θ_{ij}^k . We postulate the symmetry $e_{ij}^k = e_{ji}^k$ for theoretical convenience, and define $\omega_{ij}^k = \exp(e_{ij}^k)$ along with $\mu_i^k = \exp(e_{ii}^k) + \sum_{l \in \mathcal{N}_i} \exp(e_{il}^k)$. This setup allows P^k to be interpreted as a aggregation matrix on a weighted graph $G = (V, E, \omega^k, \mu^k)$. The aggregation matrix in GCN notably satisfies $e_{ij}^k = e_{ji}^k$. Recall the definition of node similarity measure and over-smoothing in (Rusch et al., 2023a).

Definition 2.1. (Over-smoothing) Let G be an undirected, connected graph, and $X^k \in \mathbb{R}^{n \times d}$ denote the k -th layer hidden features of an N -layer GNN defined on G . Moreover, we call $\mathcal{E} : \mathbb{R}^{n \times d} \rightarrow \mathbb{R}_{\geq 0}$ a node similarity measure if it satisfies the following axioms:

- $\exists c \in \mathbb{R}^d$ with $X(i) = c$ for all nodes $i \in V$ if and only if $\mathcal{E}(X) = 0$, for $X \in \mathbb{R}^{n \times d}$
- $\mathcal{E}(X + Y) \leq \mathcal{E}(X) + \mathcal{E}(Y)$, for all $X, Y \in \mathbb{R}^{n \times d}$

We then define over-smoothing with respect to \mathcal{E} as the layer-wise exponential convergence of the node-similarity measure \mathcal{E} to zero, that is for $k = 0, \dots, N$ and some constants $C_1, C_2 > 0$

$$\mathcal{E}(X^k) \leq C_1 e^{-C_2 k}$$

The m -th derivative energy, which is defined as

$$\mathcal{E}_m(X) := \frac{1}{n} \int_G |\nabla_\mu^m X|^2 d\mu,$$

is known to be a node similarity measure (Guan and Shi, 2025), where $m \in \mathbb{N}$. The explicit expression is as follows

$$|\nabla_\mu^m X|^2 = \begin{cases} |(-\Delta_\mu)^{\frac{m}{2}} X|^2 & \text{if } m \text{ is even} \\ |\nabla_\mu(-\Delta_\mu)^{\frac{m-1}{2}} X|^2 & \text{if } m \text{ is odd} \end{cases}$$

The case $m = 0$ is exactly measure proposed by Wu et al. (2023b), the case $m = 1$ is exactly Dirichlet energy and the case $m = 2$ will be termed as Laplacian energy. A more familiar expression for Laplacian energy is that

$$\frac{1}{n} \int_G |\Delta_\mu X|^2 d\mu = \frac{1}{n} \sum_{i \in [n]} |\Delta_\mu X(i)|^2 \mu_i.$$

We will specify $\omega_{ij} = 1$ and $\mu_i = \text{deg}_i + 1$ for Laplacian energy if there is no further specification. Recall that all these measures are equivalent (Guan and Shi, 2025).

Lemma 2.1. $G = (V, E, \omega, \mu)$ is a weighted graph. Then for any function X on the graph and all $m_1, m_2 \in \mathbb{N}$, There exist universal constants $C_1, C_2 > 0$ such that

$$C_2 \int_G |\nabla_\mu^{m_1} X|^2 d\mu \leq \int_G |\nabla_\mu^{m_2} X|^2 d\mu \leq C_1 \int_G |\nabla_\mu^{m_1} X|^2 d\mu$$

The *curse of depth*, originally formalized by Sun et al. (2025), refers to the phenomenon where deeper layers contribute negligibly to representation learning. While prior work quantified this effect using accumulated variance, we empirically observe in this work that the Laplacian energy exhibits a similar accumulation pattern, following a power-law growth. To align our analysis with the over-smoothing metric (i.e., Laplacian energy), we characterize the *curse of depth* via the *relative node similarity measure* and formally define it as follows.

Definition 2.2 (The Curse of Depth). Let \mathcal{E} be the node similarity measure as established in Definition 2.1. Consider an N -layer GNN with layer indices $k = 0, \dots, N$. We define the relative node similarity $\mathcal{R}(X^k)$ as the relative rate of change in energy:

$$\mathcal{R}(X^k) = \frac{\mathcal{E}(X^k) - \mathcal{E}(X^{k-1})}{\mathcal{E}(X^{k-1})}.$$

We say that the model suffers from the curse of depth with respect to \mathcal{E} if $\mathcal{E}(X^k)$ is a growth function in terms of k and the relative node similarity converge to zero as $k \rightarrow \infty$.

3 Pre-LN versus Post-LN

3.1 Placement of LN

We give the special expression for attention of different attention based GNNs in Table 1. We use self-attention neural network(SAN) to denote GNNs using self-attention.

Table 1: Expression of attention for different attention based GNNs

Models	e_{ij}
GCN	$e_{ij} = 1$
GAT	$e_{ij} = \text{LeakyReLU}(a^T [WX(i) WX(j)])$
SAN	$e_{ij} = \frac{1}{\sqrt{d}} KX(i) \cdot QX(j)$

For all models in this work, the encoder is composed of a dropout, and a MLP. The decoder is only a MLP without activation.

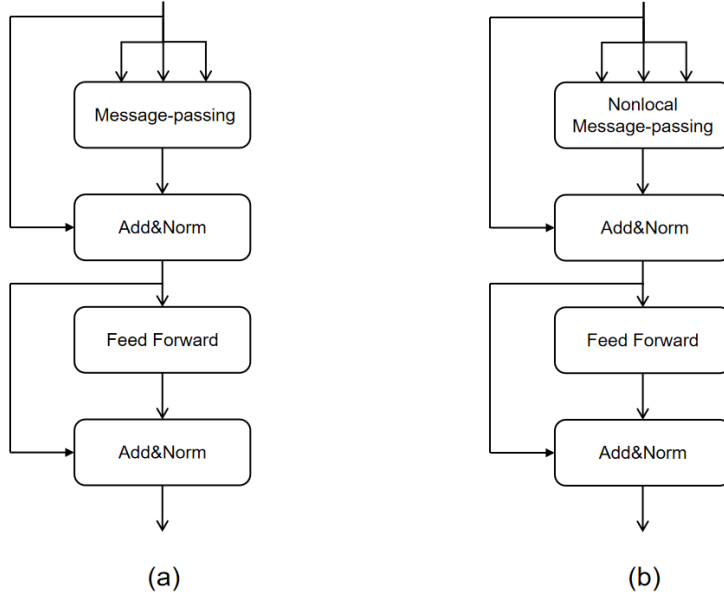


Figure 3: (a) The Post-LN model. (b) Our proposed nonlocal model with Post-LN.

Hidden layers A single hidden layer of Post-LN architecture is depicted in the Figure 3(a). The update formula in message-passing step of Post-LN model is that

$$\mathbf{MP}(X^k) = (P_1^k X^k V_1^k \parallel P_2^k X^k V_2^k \parallel \dots \parallel P_h^k X^k V_h^k) W^k,$$

where h is the number of attention heads, V_i^k and W^k are learnable matrices. The overall formula of hidden layer is that

$$\begin{aligned} Y^k &= \mathbf{Norm}(X^k + \mathbf{MP}(X^k)) \\ \tilde{Y}^k &= \mathbf{FFN}(Y^k) \\ X^{k+1} &= \mathbf{Norm}(Y^k + \tilde{Y}^k) \end{aligned}$$

Pre-LN is much used in modern LLMs, For the Pre-LN model the position of layer normalization is putted forward. The overall formula for Pre-LN model is as follows

$$\begin{aligned} Y^k &= X^k + \mathbf{MP}(\mathbf{Norm}(X^k)) \\ X^{k+1} &= Y^k + \mathbf{FFN}(\mathbf{Norm}(Y^k)) \end{aligned}$$

3.2 Analysis of over-smoothing

In this subsection, we empirically demonstrate that the Pre-LN SAN architecture is robust to over-smoothing, whereas the Post-LN counterpart is susceptible to it. We focus on the task of fully supervised node classification. To systematically analyze the impact of depth, we evaluate Pre-LN SANs with varying network depths selected from $\{2, 32, 64, 128, 256\}$. Detailed training configurations are provided in the Appendix B.1. Our experiments are conducted on five standard benchmark datasets: Cora, Citeseer, and Pubmed (Yang et al., 2016), as well as Coauthor CS and Coauthor Physics (Shchur et al., 2019). For all datasets, we employ a random split of 60%/20%/20% for training, validation, and testing, respectively.

To characterize the intrinsic dynamical behavior of the architecture prior to optimization, the following table presents the Laplacian energy of the final-layer output for the **untrained** SAN with Pre-LN.

Table 4: The Laplacian energy of Post-LN SAN at initialization

Layers Datasets	2 Layers	32 Layers	64 Layers	128 Layers	256 Layers
Cora	0.558	1.04×10^{-5}	2.10×10^{-6}	3.82×10^{-7}	1.32×10^{-12}
Citeseer	0.301	1.14×10^{-5}	6.29×10^{-7}	6.29×10^{-7}	1.17×10^{-12}
Pubmed	2.41×10^{-2}	4.08×10^{-6}	2.57×10^{-7}	4.62×10^{-9}	7.55×10^{-12}
Physics	0.379	4.10×10^{-5}	2.30×10^{-7}	1.04×10^{-9}	7.40×10^{-14}
CS	1.40	3.71×10^{-5}	6.60×10^{-6}	2.57×10^{-7}	3.10×10^{-13}

Table 5: Accuracy of Post-LN SAN on Cora

Layers Sets	2 Layers Acc	32 Layers Acc	64 Layers Acc	128 Layers Acc	256 Layers Acc
Training set	97.11	91.32	96.06	84.11	31.65
Validation set	86.14	85.77	85.77	77.82	29.57
Test set	87.66	86.19	86.74	81.58	29.83

Table 2: The Laplacian energy of Pre-LN SAN at initialization

Layers Datasets	2 Layers	32 Layers	64 Layers	128 Layers	256 Layers
Cora	1.70	6.56	9.86	23.69	23.23
Citeseer	1.24	5.91	8.24	11.69	14.61
Pubmed	0.116	0.194	0.229	0.381	0.404
Physics	1.55	6.38	9.72	18.82	31.18
CS	6.96	39.97	44.41	67.75	104.23

As evidenced in the table, the Laplacian energy exhibits a consistent increase as network depth grows. This trend indicates that SAN with Pre-LN effectively prevents the over-smoothing issue typically observed in deep GNNs. In terms of classification performance, we report the training, validation, and test accuracies corresponding to the epoch with the highest validation accuracy (i.e., peak validation performance). Table 3 details the results for the Cora dataset. Due to space constraints, the experimental results for the remaining four datasets are provided in the Appendix B.3.

Table 3: Accuracy of Pre-LN SAN on Cora

Layers Sets	2 Layers Acc	32 Layers Acc	64 Layers Acc	128 Layers Acc	256 Layers Acc
Training set	100	99.08	93.97	97.23	100
Validation set	86.32	86.51	86.69	87.43	87.80
Test set	88.40	87.11	88.03	86.92	87.29

We observe that the model maintains trainability, showing no degradation in training or validation accuracy.

We now turn our attention to the Post-LN SAN configuration. Following the same experimental protocol, we train models with depths $L \in \{2, 32, 64, 128, 256\}$; full training details are provided in the Appendix B.1. Table 4 presents the Laplacian energy of the outputs for these **untrained** models. Additionally, Table 5 reports the classification performance (training, validation, and test accuracy) corresponding to the best validation checkpoint. We report results of Cora here and put others in the Appendix B.3. As evident from the results, the Laplacian energy undergoes an exponential decay with increasing depth, signifying severe over-smoothing of the node features. This feature collapse precipitates a rapid degradation in model performance. Crucially, accuracy drops precipitously not only on the test set but also on the training and validation sets. This indicates that the deep Post-

LN architecture suffers from fundamental optimization difficulties, rendering the model effectively untrainable in deeper regimes.

Also, we compare a 256-layer Pre-LN SAN with a 256-layer Post-LN SAN. As illustrated in Figure 1(a)(c), the Laplacian energy of the layer outputs X^k in the Pre-LN SAN increases. In contrast, the Post-LN SAN exhibits an exponential decrease in Laplacian energy across layers. This suggests that Pre-LN SANs are biased towards the identity branch, primarily accumulating Laplacian energy while exhibiting diminishing relative changes in deeper layers, which leads to inefficient depth utilization. Conversely, the Post-LN architecture—which applies normalization after the residual addition—effectively mixes information from both the residual and identity branches. However, this aggressive mixing can lead to over-smoothing in deep GNNs.

4 Understand and Overcome over-smoothing

4.1 Theoretical analysis

For Post-LN models, LN plays a role in mixing information of residual branch and identity branch. Over-smoothing is caused by residual branch, hence we can simply consider attention based GNNs. Recall that attention based GNNs can be viewed as the discretization of heat equation (Wang et al., 2021)

$$\frac{\partial X_t}{\partial t} = \Delta_\mu X_t.$$

We recall the reason behind the over-smoothing which is presented in (Guan and Shi, 2025). Under the heat equation, the Dirichlet energy will evolve as follows.

$$\frac{\partial \int_G |\nabla_\mu X_t|^2 d\mu}{\partial t} = -2 \int_G |\Delta_\mu X_t|^2 d\mu.$$

By Lemma 2.1, for some constant C_1, C_2 we have

$$C_1 \int_G |\nabla_\mu X_t|^2 d\mu \leq \int_G |\Delta_\mu X_t|^2 d\mu \leq C_2 \int_G |\nabla_\mu X_t|^2 d\mu$$

Then

$$-2C_2 \int_G |\nabla_\mu X_t|^2 d\mu \leq \frac{\partial \int_G |\nabla_\mu X_t|^2 d\mu}{\partial t} \leq -2C_1 \int_G |\nabla_\mu X_t|^2 d\mu$$

solving this we have

$$-2C_2 \leq \frac{\partial (\ln(\int_G |\nabla_\mu X_t|^2 d\mu))}{\partial t} \leq -2C_1.$$

Hence, we have

$$e^{-2C_2 t} \int_G |\nabla_\mu X_0|^2 d\mu \leq \int_G |\nabla_\mu X_t|^2 d\mu \leq e^{-2C_1 t} \int_G |\nabla_\mu X_0|^2 d\mu.$$

By above heuristic computation, if under some evolving equation we have

$$\frac{\int_G |\nabla_\mu X_t|^2 d\mu}{\partial t} \sim -(\int_G |\nabla_\mu X_t|^2 d\mu)^\beta$$

for some $\beta > 1$, then we have

$$\frac{\partial}{\partial t} \left(\frac{1}{(\int_G |\nabla_\mu X_t|^2 d\mu)^{\beta-1}} \right) \sim 1.$$

Hence, solving this we will have the algebraically decay rate with some constants $C_1, C_2 > 0$.

$$\min(C_2 \int_G |\nabla_\mu X_0|^2 d\mu, C_2 \frac{1}{t^{\frac{1}{\beta-1}}}) \leq \int_G |\nabla_\mu X_t|^2 d\mu \leq C_1 \frac{1}{t^{\frac{1}{\beta-1}}}.$$

When $\beta \rightarrow 1$, the decay rate will be faster than any algebraically decay rate which is exactly exponentially decay rate. In the next theorem, we give a simple evolving equation which can achieve our goal for $\beta = 2$.

Theorem 4.1. Let $G = (V, E, \omega, \mu)$ be a finite graph, $X_0 \in \mathbb{R}^{n \times d}$ is the initial feature, then under the non-local diffusion

$$\frac{\partial X_t}{\partial t} = \left(\int_G |\Delta_\mu X_t|^2 d\mu \right) \Delta_\mu X_t$$

we have the algebraically decay rate

$$\min(C_2 \int_G |\nabla_\mu X_0|^2 d\mu, C_2 \frac{1}{t}) \leq \int_G |\nabla_\mu X_t|^2 d\mu \leq C_1 \frac{1}{t}.$$

We now present our Nonlocal Message-passing Algorithm.

Architecture of nonlocal message passing with Post-LN The architecture of hidden layers is shown in Figure3(b). Our nonlocal model with Pos-LN only differs in the message-passing step which is called nonlocal message passing. That is

$$\text{NonlocalMP}(X^k) = \left(\frac{1}{n} \|P_1^k X^k - X^k\|^2 P_1^k X^k V_1^k \left\| \dots \left\| \frac{1}{n} \|P_h^k X^k - X^k\|^2 P_h^k X^k V_h^k \right\| \right) W^k.$$

That is we multiply Laplacian energy $\frac{1}{n} \|P_i^k X^k - X^k\|^2$ before each aggregation $P_i^k X^k$ Intuitively, If over-smoothing occurs and Laplacian energy $\frac{1}{n} \|P_i^k X^k - X^k\|^2$ is every small, then the residual branch $\frac{1}{n} \|P_i^k X^k - X^k\|^2 P_i^k X^k V^k$ will be small at the same time, hence aggregation term $P_i^k X^k$ do not influence much.

Computational complexity of our proposed method Since $P_i^k X^k$ is already computed, the extra computation of Laplacian energy only require $O(nd)$.

4.2 Empirical analysis

In this subsection, we provide empirical evidence that our proposed method effectively mitigates the over-smoothing issue. Adopting a consistent experimental setting, we report the Laplacian energy at initialization and the classification accuracy corresponding to the best-performing model on the validation set. Due to space limitations, we present the results on the Cora dataset here as a representative example, while detailed results for the remaining datasets are provided in the Appendix B.4.

Table 6: The Laplacian energy of nonlocal SAN with Post-LN at initialization

Layers Datasets	2 Layers	32 Layers	64 Layers	128 Layers	256 Layers
Cora	0.793	6.47×10^{-3}	2.36×10^{-3}	1.28×10^{-3}	8.55×10^{-5}
Citeseer	0.489	8.43×10^{-3}	2.58×10^{-3}	2.91×10^{-3}	4.39×10^{-5}
Pubmed	3.56×10^{-2}	1.98×10^{-3}	1.55×10^{-3}	5.91×10^{-5}	2.13×10^{-5}
Physics	0.812	7.71×10^{-3}	2.64×10^{-3}	2.70×10^{-3}	1.04×10^{-4}
CS	3.26	3.13×10^{-2}	1.65×10^{-2}	4.72×10^{-3}	3.04×10^{-4}

Table 7: Accuracy of nonlocal SAN with Post-LN on Cora

Layers Sets	2 Layers Acc	32 Layers Acc	64 Layers Acc	128 Layers Acc	256 Layers Acc
Training set	100	92.98	91.69	90.89	92.12
Validation set	85.77	87.62	86.14	87.43	85.40
Test set	88.77	87.29	87.11	88.03	87.85

We observe that the Laplacian energy decays gradually. Crucially, unlike Post-LN SAN, our proposed nonlocal SAN with Post-LN facilitates trainability in deeper layers.

5 Analysis of the curse of depth

While modern LLMs predominantly adopt Pre-LN to mitigate issues such as gradient instability, recent studies suggest that Pre-LN Transformers may suffer from inefficient depth utilization. (Csordás et al., 2025) analyzed models including Llama 3.1, Qwen 3, and QLMo 2, measuring the contribution norm of each layer relative to the residual stream. They observed that beyond the middle layers, the models tend to amplify existing features rather than substantially modifying the residual stream, resulting in diminishing representation updates in deeper layers. Similar phenomena in the Qwen 2.5 family have been reported by (Hu et al., 2025).

(Sun et al., 2025) formalized this limitation as the ‘curse of depth’ in LLMs, which refers to the marginal contribution of deeper layers to both learning and representation. By performing layer pruning without fine-tuning, they demonstrated that removing deeper layers in Pre-LN models (e.g., Qwen 3) incurs only minor performance drops—or even performance gains—whereas Post-LN models (e.g., BERT) suffer significant degradation. Furthermore, analysis of the angular distance between layer representations revealed that deeper layers in Pre-LN models produce outputs highly similar to their preceding layers, indicating a high degree of redundancy.

In this section, we provide empirical evidence within the context of GNNs, corroborating the findings of (Sun et al., 2025). Figure 2 presents the cosine similarity between layer representations. For two layer representations $X^s, X^t \in \mathbb{R}^{n \times d}$, the cosine similarity is defined as:

$$\text{sim}(X^s, X^t) = \frac{1}{n} \sum_{i \in [n]} \frac{X^s(i) \cdot X^t(i)}{|X^s(i)| |X^t(i)|}. \tag{1}$$

In the non-local SAN with Post-LN, representations from distant layers display low similarity, indicating continuous feature transformation. In contrast, deeper layers in the Pre-LN SAN exhibit increasingly high similarity, reinforcing the hypothesis of reduced effective feature transformation in deep Pre-LN models.

Also, we perform a layer sensitivity analysis to assess the impact of specific layers on the final output. We prune individual layers from the set $\{2, 32, 64, 96, 128, 160, 192, 244\}$ and evaluate the resulting test accuracy, as detailed in Table 8. For the nonlocal SAN with Post-LN, pruning any intermediate layer leads to a degradation in accuracy compared to the baseline of 87.85%, implying that all layers contribute to the learned representation. Strikingly, for the Pre-LN model, pruning layers beyond depth 64 has a negligible impact on accuracy. This finding indicates that deep layers in the Pre-LN architecture contribute minimally to the final representation, effectively validating the existence of the ‘curse of depth’

Table 8: Impact of pruning individual layers on the accuracy(Cora)

Layers methods	2 Acc	32 Acc	64 Acc	96 Acc	128 Acc	160 Acc	192 Acc	224 Acc
nonlocal SAN with Post-LN	87.66	87.11	86.74	86.92	87.29	87.11	86.92	87.66
Pre-LN SAN	81.58	86.56	87.29	87.29	87.29	87.29	87.29	87.29

Complementing the aforementioned layer sensitivity analysis, we further characterize the *curse of depth* via the power-law growth of the relative Laplacian energy. we already give a definition for the curse of depth in Definition 2.1. As illustrated in Figure 1(c), the evolution of Laplacian energy exhibits a near-linear trend on a log-log scale, indicative of power-law growth. Corroborating evidence for additional datasets is provided in the Appendix C. Hence these results validate our definition. Theoretically, we can derive an estimate of decat rate of relative Laplacian energy for the continuous formulation of Pre-LN models in Theorem 5.1.

Theorem 5.1. *For the evolving equation*

$$\frac{\partial X_t}{\partial t} = P_\mu(\text{Norm}(X_t))$$

There exist constant $C_1 > 0$ such that we have $\int_G |\nabla X_t|^2 d\mu \leq (C_1 t + \sqrt{\int_G |\nabla_\mu X_0|^2 d\mu})^2$. Furthermore, assuming a power-law lower bound for $\int_G |\nabla_\mu X_t|^2 d\mu$

$$C_2 t^q \leq \int_G |\nabla_\mu X_t|^2 d\mu,$$

we can get a power-law decay for relative energy

$$\frac{1}{\int_G |\nabla_\mu X_t|^2 d\mu} \frac{\partial \int_G |\nabla_\mu X_t|^2 d\mu}{\partial t} \leq C \frac{1}{t^{\frac{q}{2}}}.$$

6 Conclusion

We develop a simple method called nonlocal message passing to theoretically and empirically overcome over-smoothing efficiently. This method can be also easily applied to any problem with respect to exponentially converge to steady state. Also, the distinct phenomenon shed light to addressing the curse of depth in LLMs and further study on Post-LN configuration in LLMs. Most importantly, more works need to be done in the future to train a large and universal graph neural networks.

References

- Besta, M., Grob, R., Miglioli, C., Bernold, N., Kwasniewski, G., Gjini, G., Kanakagiri, R., Ashkboos, S., Gianinazzi, L., Dryden, N., et al. (2022). Motif prediction with graph neural networks. In *Proceedings of the 28th ACM SIGKDD conference on knowledge discovery and data mining*, pages 35–45.
- Cai, C. and Wang, Y. (2020). A note on over-smoothing for graph neural networks.
- Chamberlain, B. P., Rowbottom, J., Gorinova, M. I., Webb, S. D., Rossi, E., and Bronstein, M. M. (2021). GRAND: Graph neural diffusion. In *The Symbiosis of Deep Learning and Differential Equations*.
- Chen, M., Wei, Z., Huang, Z., Ding, B., and Li, Y. (2020a). Simple and deep graph convolutional networks. In *International conference on machine learning*, pages 1725–1735. PMLR.
- Chen, M., Wei, Z., Huang, Z., Ding, B., and Li, Y. (2020b). Simple and deep graph convolutional networks. In *Proceedings of the 37th International Conference on Machine Learning, ICML’20*. JMLR.org.
- Csordás, R., Manning, C. D., and Potts, C. (2025). Do language models use their depth efficiently?
- Fan, W., Ma, Y., Li, Q., He, Y., Zhao, E., Tang, J., and Yin, D. (2019). Graph neural networks for social recommendation. In *The world wide web conference*, pages 417–426.
- Geshkovski, B., Letrouit, C., Polyanskiy, Y., and Rigollet, P. (2025). A mathematical perspective on transformers.
- Guan, W. and Shi, Z. (2025). Measuring over-smoothing beyond dirichlet energy.
- Hu, Y., Zhou, C., and Zhang, M. (2025). What affects the effective depth of large language models? In *Mechanistic Interpretability Workshop at NeurIPS 2025*.
- Joshi, C. K. (2025). Transformers are graph neural networks.
- Kang, Q., Zhao, K., Ding, Q., Ji, F., Li, X., Liang, W., Song, Y., and Tay, W. P. (2024). Unleashing the potential of fractional calculus in graph neural networks with FROND. In *The Twelfth International Conference on Learning Representations*.
- Kipf, T. N. and Welling, M. (2017). Semi-supervised classification with graph convolutional networks. In *International Conference on Learning Representations*.

- Luo, Y., Shi, L., and Wu, X.-M. (2024). Classic gnns are strong baselines: Reassessing gnns for node classification.
- Oono, K. and Suzuki, T. (2020). Graph neural networks exponentially lose expressive power for node classification. In *International Conference on Learning Representations*.
- Rampášek, L., Galkin, M., Dwivedi, V. P., Luu, A. T., Wolf, G., and Beaini, D. (2023). Recipe for a general, powerful, scalable graph transformer.
- Rusch, T. K., Bronstein, M. M., and Mishra, S. (2023a). A survey on oversmoothing in graph neural networks.
- Rusch, T. K., Chamberlain, B., Rowbottom, J., Mishra, S., and Bronstein, M. (2022). Graph-coupled oscillator networks. In Chaudhuri, K., Jegelka, S., Song, L., Szepesvari, C., Niu, G., and Sabato, S., editors, *Proceedings of the 39th International Conference on Machine Learning*, volume 162 of *Proceedings of Machine Learning Research*, pages 18888–18909. PMLR.
- Rusch, T. K., Chamberlain, B. P., Mahoney, M. W., Bronstein, M. M., and Mishra, S. (2023b). Gradient gating for deep multi-rate learning on graphs. In *The Eleventh International Conference on Learning Representations*.
- Scholkemper, M., Wu, X., Jadbabaie, A., and Schaub, M. T. (2025). Residual connections and normalization can provably prevent oversmoothing in gnns.
- Shchur, O., Mumme, M., Bojchevski, A., and Günnemann, S. (2019). Pitfalls of graph neural network evaluation.
- Shi, H., GAO, J., Xu, H., Liang, X., Li, Z., Kong, L., Lee, S. M. S., and Kwok, J. (2022). Revisiting over-smoothing in BERT from the perspective of graph. In *International Conference on Learning Representations*.
- Shirzad, H., Vellingker, A., Venkatachalam, B., Sutherland, D. J., and Sinop, A. K. (2023). Exphormer: Sparse transformers for graphs.
- Sun, W., Song, X., Li, P., Yin, L., Zheng, Y., and Liu, S. (2025). The curse of depth in large language models.
- Vaswani, A., Shazeer, N., Parmar, N., Uszkoreit, J., Jones, L., Gomez, A. N., Kaiser, L., and Polosukhin, I. (2017). Attention is all you need. In *Proceedings of the 31st International Conference on Neural Information Processing Systems, NIPS’17*, page 6000–6010, Red Hook, NY, USA. Curran Associates Inc.
- Veličković, P., Cucurull, G., Casanova, A., Romero, A., Liò, P., and Bengio, Y. (2018). Graph attention networks. In *International Conference on Learning Representations*.
- Wang, Q., Li, B., Xiao, T., Zhu, J., Li, C., Wong, D. F., and Chao, L. S. (2019). Learning deep transformer models for machine translation. *arXiv preprint arXiv:1906.01787*.
- Wang, Y., Wang, Y., Yang, J., and Lin, Z. (2021). Dissecting the diffusion process in linear graph convolutional networks. In Beygelzimer, A., Dauphin, Y., Liang, P., and Vaughan, J. W., editors, *Advances in Neural Information Processing Systems*.
- Wu, F., Souza, A., Zhang, T., Fifty, C., Yu, T., and Weinberger, K. (2019). Simplifying graph convolutional networks. In Chaudhuri, K. and Salakhutdinov, R., editors, *Proceedings of the 36th International Conference on Machine Learning*, volume 97 of *Proceedings of Machine Learning Research*, pages 6861–6871. PMLR.
- Wu, Q., Zhao, W., Li, Z., Wipf, D., and Yan, J. (2023a). Nodeformer: A scalable graph structure learning transformer for node classification.
- Wu, X., Ajorlou, A., Wu, Z., and Jadbabaie, A. (2023b). Demystifying oversmoothing in attention-based graph neural networks. In Oh, A., Naumann, T., Globerson, A., Saenko, K., Hardt, M., and Levine, S., editors, *Advances in Neural Information Processing Systems*, volume 36, pages 35084–35106. Curran Associates, Inc.

Yang, Z., Cohen, W. W., and Salakhutdinov, R. (2016). Revisiting semi-supervised learning with graph embeddings.

Zhao, L. and Akoglu, L. (2020). Pairnorm: Tackling oversmoothing in gnns. In *International Conference on Learning Representations*.

A Proofs of Theorems

A.1 Preliminaries

We first give an integration by parts lemma.

Lemma A.1. *Let $G = (V, E, \omega, \mu)$ be a weighted graph, then we have integration by parts*

$$\int_G -\Delta_\mu X \cdot Y d\mu = \int_G \nabla_\mu X \cdot \nabla_\mu Y d\mu$$

Proof. Given a weighted graph $G = (V, E, \omega, \mu)$ and vectored-valued functions $X, Y : V \rightarrow \mathbb{R}^d$. First, we suppose $d = 1$, we have the following equality

$$\begin{aligned} & \sum_{i \in [n]} \sum_{j \in \mathcal{N}_i} \omega_{ij} X(i) Y(i) \\ &= \sum_{i \sim j} \omega_{ij} (X(i) Y(i) + X(j) Y(j)) \\ &= \sum_{i \in [n]} \sum_{j \in \mathcal{N}_i} \omega_{ij} X(j) Y(j) \end{aligned}$$

and

$$\begin{aligned} & \sum_{i \in [n]} \sum_{j \in \mathcal{N}_i} \omega_{ij} X(j) Y(i) \\ &= \sum_{i \sim j} \omega_{ij} (X(j) Y(i) + X(i) Y(j)) \\ &= \sum_{i \in [n]} \sum_{j \in \mathcal{N}_i} \omega_{ij} X(i) Y(j) \end{aligned}$$

Combining above equalities we deduce

$$\begin{aligned} \int_V \Delta_\mu X \cdot Y d\mu &= \sum_{i=1}^n \sum_{j \in \mathcal{N}_i} \omega_{ij} (X(j) - X(i)) Y(i) \\ &= \sum_{i=1}^n \sum_{j \in \mathcal{N}_i} (\omega_{ij} X(j) Y(i) - \omega_{ij} X(i) Y(i)) \\ &= \sum_{i=1}^n \sum_{j \in \mathcal{N}_i} (\omega_{ij} X(i) Y(j) - \omega_{ij} X(j) Y(j)) \\ &= \sum_{i=1}^n \sum_{j \in \mathcal{N}_i} \omega_{ij} (X(i) - X(j)) Y(j) \end{aligned}$$

Thus adding the right-hand side of the first line and last line we get

$$\begin{aligned} \int_G \Delta_\mu X \cdot Y d\mu &= \sum_{i=1}^n \sum_{j \in \mathcal{N}_i} \frac{\omega_{ij}}{2} (X(j) - X(i)) (Y(i) - Y(j)) \\ &= - \int_V \nabla_\mu X \cdot \nabla_\mu Y \end{aligned}$$

Now suppose general d and $X = (X_1, \dots, X_d)^T, Y = (Y_1, \dots, Y_d)^T$, then a direct calculation yield

$$\begin{aligned}
& \int_G \Delta_\mu X \cdot Y d\mu \\
&= \int_G \Delta_\mu X_1 \cdot Y_1 d\mu + \dots + \Delta_\mu X_d \cdot Y_d d\mu \\
&= - \int_G \nabla_\mu X_1 \cdot \nabla_\mu Y_1 d\mu - \dots - \nabla_\mu X_d \cdot \nabla_\mu Y_d d\mu \\
&= - \int_G \nabla_\mu X \cdot \nabla_\mu Y d\mu
\end{aligned}$$

□

A.2 Supplemental proof of subsection 4.1

We only need to prove

$$\frac{\partial \int_G |\nabla_\mu X_t|^2 d\mu}{\partial t} = - \int_G |\Delta_\mu X_t|^2 d\mu.$$

This is from Lemma A.1 and a direct computation.

$$\begin{aligned}
\frac{\partial \int_G |\nabla_\mu X_t|^2 d\mu}{\partial t} &= -2 \int_G \Delta_\mu X_t \cdot \frac{\partial X_t}{\partial t} d\mu \\
&= -2 \int_G |\Delta_\mu X_t|^2 d\mu
\end{aligned}$$

A.3 Proof of Theorem 4.1

We only need to prove that for some constants $C_1, C_2 > 0$ we have

$$-C_1 \left(\int_G |\nabla_\mu X_t|^2 d\mu \right)^2 \leq \frac{\int_G |\nabla_\mu X_t|^2 d\mu}{\partial t} \sim -C_2 \left(\int_G |\nabla_\mu X_t|^2 d\mu \right)^2$$

Similarly by Lemma A.1 we have

$$\begin{aligned}
\frac{\partial \int_G |\nabla_\mu X_t|^2 d\mu}{\partial t} &= -2 \int_G \Delta_\mu X_t \cdot \frac{\partial X_t}{\partial t} d\mu \\
&= -2 \left(\int_G |\Delta_\mu X_t|^2 d\mu \right)^2.
\end{aligned}$$

Since there exists constants $C_1, C_2 > 0$ such that

$$C_1 \int_G |\nabla_\mu X_t|^2 d\mu \leq \int_G |\Delta_\mu X_t|^2 d\mu \leq C_2 \int_G |\nabla_\mu X_t|^2 d\mu$$

We have the desired results.

A.4 Proof of Theorem 5.1

Suppose the l^2 eigenvalues of operator $-\Delta_\mu : \mathbb{R}^{n \times d} \rightarrow \mathbb{R}^{n \times d}$ are

$$\lambda_1, \dots, \lambda_{nd}$$

and the corresponding eigenfunctions

$$f_1, \dots, f_{nd}$$

for fixed t suppose the spectral decomposition of X_t is

$$X_t = \sum_i C_i f_i$$

the spectral decomposition of $Norm(X_t)$ is

$$Norm(X_t) = \sum_i B_i f_i$$

then we have

$$\begin{aligned}
\frac{\partial \int_G |\nabla_\mu X_t|^2 d\mu}{\partial t} &= \int_G -P_\mu \Delta_\mu X_t \cdot \text{proj}_{S^d} X_t d\mu \\
&= \sum_i (1 + \lambda_i) \lambda_i B_i C_i \\
&\leq C \sum_i \sqrt{\lambda_i} |B_i C_i| \\
&\leq C \sqrt{\left(\sum_i B_i^2\right) \left(\sum_i \lambda_i C_i^2\right)}
\end{aligned}$$

Since

$$\sum_i \lambda_i C_i^2 = \int_G |\nabla_\mu X_t|^2 d\mu$$

and

$$\sum_i B_i^2 = \int_G |\text{Norm}(X_t)|^2 d\mu = n$$

Hence

$$\frac{\partial \int_G |\nabla_\mu X_t|^2 d\mu}{\partial t} \leq C \sqrt{\int_G |\nabla_\mu X_t|^2 d\mu}$$

solving this we have

$$\int_G |\nabla_\mu X_t|^2 d\mu \leq (C_1 t + \sqrt{\int_G |\nabla_\mu X_0|^2 d\mu})^2$$

Now assuming a lower power-law bound

$$C_2 t^q \leq \int_G |\nabla_\mu X_t|^2 d\mu,$$

For the relative Laplacian energy, we directly compute that

$$\frac{1}{\int_G |\nabla_\mu X_t|^2 d\mu} \frac{\partial \int_G |\nabla_\mu X_t|^2 d\mu}{\partial t} \leq \frac{C}{\sqrt{\int_G |\nabla_\mu X_t|^2 d\mu}} \leq \frac{C}{t^{\frac{q}{2}}}.$$

B Experiment details

B.1 Experiment Setup

For all models, we train 5000 epoches and the L2 regularization is 5e-4. Hidden dimension is fixed as 32. For Pre-LN, the learning rate is fixed as 1e-3. For Post-LN, we use the warm up strategy for learning rate with maximum 1e-4.

B.2 Data details

Table 9: Dataset Statistics

Datasets	Cora	Citeseer	Pubmed	CS	Physics
Nodes	2708	3327	19717	18333	34493
Edges	5278	4522	44324	81894	247962
Features	1433	3703	500	6805	8415
Classes	7	6	3	15	5

B.3 Supplemental results in subsection 3.2

The training, validation and test accuracy of SAN with Pre-LN are as follow.

Table 10: Train accuracy of SAN with Pre-LN over different datasets

Layers Datasets	2 Layers Acc	32 Layers Acc	64 Layers Acc	128 Layers Acc	256 Layers Acc
Cora	100	99.08	93.97	97.23	100
Citeseer	100	89.98	100	99.90	89.23
Pubmed	94.51	97.02	99.64	97.44	97.43
Physics	100	100	98.51	99.64	99.45
CS	100	97.44	99.99	98.17	97.78

Table 11: Validation accuracy of Transformer with Pre-LN

Layers Datasets	2 Layers Acc	32 Layers Acc	64 Layers Acc	128 Layers Acc	256 Layers Acc
Cora	86.32	86.51	86.69	87.43	87.80
Citeseer	74.44	75.64	75.04	73.53	73.98
Pubmed	90.03	89.35	89.45	89.78	89.78
Physics	97.14	96.58	96.71	96.36	96.78
CS	94.38	92.55	92.06	92.03	92.39

Table 12: Test accuracy of SAN with Pre-LN

Layers Datasets	2 Layers Acc	32 Layers Acc	64 Layers Acc	128 Layers Acc	256 Layers Acc
Cora	88.40	87.11	88.03	86.92	87.29
Citeseer	72.07	72.37	70.87	71.17	72.67
Pubmed	89.00	89.40	88.39	89.17	89.43
Physics	96.64	96.09	96.16	95.70	96.26
CS	94.77	93.29	92.64	92.53	93.21

The training, validation and test accuracy of SAN with Post-LN are as follow.

Table 13: Train accuracy of SAN with Post-LN over different datasets

Layers Datasets	2 Layers Acc	32 Layers Acc	64 Layers Acc	128 Layers Acc	256 Layers Acc
Cora	97.11	91.32	96.06	84.11	31.65
Citeseer	94.49	88.03	90.48	86.02	55.96
Pubmed	97.13	85.75	85.16	70.14	40.18
Physics	100	97.36	95.23	76.12	50.84
CS	100	94.53	92.36	75.66	23.14

Table 14: Validation accuracy of Transformer with Post-LN over different datasets

Layers Datasets	2 Layers Acc	32 Layers Acc	64 Layers Acc	128 Layers Acc	256 Layers Acc
Cora	86.14	85.77	85.77	77.82	29.57
Citeseer	74.74	72.93	75.49	73.98	54.59
Pubmed	89.88	83.87	84.02	70.94	39.23
Physics	96.74	95.42	94.61	76.37	50.13
CS	93.51	89.77	89.33	76.32	24.99

Table 15: Accuracy of SAN with Post-LN

Layers Datasets	2 Layers Acc	32 Layers Acc	64 Layers Acc	128 Layers Acc	256 Layers Acc
Cora	87.66	86.19	86.74	81.58	29.83
Citeseer	73.12	71.62	71.77	70.42	51.65
Pubmed	89.55	83.62	83.01	71.15	39.93
Physics	96.39	94.58	94.19	75.77	49.96
CS	94.06	90.79	89.59	76.23	23.39

B.4 Supplemental results in subsection 4.2

The training, validation and test accuracy of nonlocal SAN with Post-LN are as follow.

Table 16: Train accuracy of nonlocal SAN with Post-LN

Layers Datasets	2 Layers Acc	32 Layers Acc	64 Layers Acc	128 Layers Acc	256 Layers Acc
Cora	100	92.98	91.69	90.89	89.35
Citeseer	99.25	87.93	87.68	89.38	89.43
Pubmed	95.84	96.98	93.92	95.00	95.13
Physics	100	97.70	95.95	94.07	98.10
CS	100	95.60	94.91	95.53	94.67

Table 17: validation accuracy of nonlocal SAN with Post-LN

Layers Datasets	2 Layers Acc	32 Layers Acc	64 Layers Acc	128 Layers Acc	256 Layers Acc
Cora	85.77	87.62	86.14	87.43	87.25
Citeseer	73.23	72.78	73.68	72.78	73.53
Pubmed	90.29	89.04	87.67	87.98	87.60
Physics	96.88	95.49	95.22	93.53	95.42
CS	93.92	90.48	90.78	90.75	89.91

Table 18: Test accuracy of nonlocal SAN with Post-LN

Layers Datasets	2 Layers Acc	32 Layers Acc	64 Layers Acc	128 Layers Acc	256 Layers Acc
Cora	88.77	87.29	87.11	88.03	87.85
Citeseer	69.22	71.77	72.52	71.32	71.62
Pubmed	89.58	88.79	87.45	88.24	87.53
Physics	96.45	94.84	94.39	93.32	94.99
CS	94.27	91.09	91.22	91.47	90.68

C The curse of depth

For Pre-LN SAN, we give the evolution of Laplacian energy on Citeseer, Pubmed, CS, Physics at initialization as follow

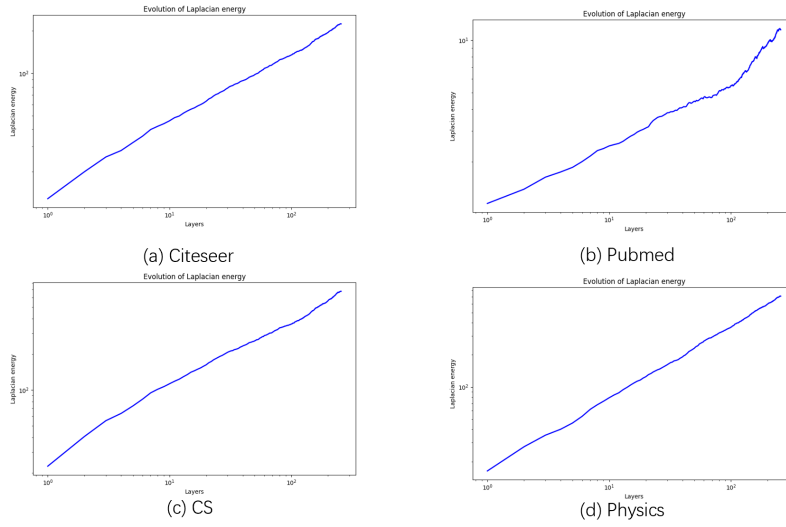


Figure 4: Evolution of Laplacian energy at initialization.